Journal Name

Dynamic Article Links ►

Cite this: DOI: 10.1039/c0xx00000x

www.rsc.org/xxxxxx

ARTICLE TYPE

Vapour-adsorption and chromic behaviours of luminescent coordination polymers composed of a Pt(II)-diimine metalloligand and alkaline-earth metal ions

Hirofumi Hara,[a] Atsushi Kobayashi,*[a] Shin-ichiro Noro,[b] Ho-Chol Chang[a] and Masako Kato*[a]

Received (in XXX, XXX) Xth XXXXXXXXX 20XX, Accepted Xth XXXXXXXXX 20XX
DOI: 10.1039/b000000x

Four new bimetallic coordination polymers (CPs), $\{M[Pt(CN)_2(5,5'\text{-dcbpy})]\cdot 4H_2O\}_n$ (M = Mg^{2+}, Ca^{2+}, Sr^{2+}, Ba^{2+}; 5,5′-H_2dcbpy = 5,5′-dicarboxy-2,2′-bipyridine) were synthesized using four alkaline-earth metal ions and a Pt(II)-diimine metalloligand [$Pt(CN)_2$(5,5′-H_2dcbpy)]. All four CPs are isomorphous with the Zn complex, $\{Zn[Pt(CN)_2(5,5'\text{-dcbpy})]\cdot 4H_2O\}_n$, which exhibits effective metallophilic interaction between Pt(II) ions. These CPs exhibited colourful thermochromic behaviour and solid-state solvatochromic-like behaviours when suspended in various solvents. Thermogravimetric analysis and vapour-adsorption measurements revealed that the CPs can reversibly adsorb water and MeOH vapours. The emission energy of the triplet metal-metal-to-ligand charge-transfer (^{3}MMLCT) state varied markedly upon guest adsorption/desorption. The chromic and vapour-adsorption properties of these CPs depend strongly on the cross-linking M^{2+} ions.

Introduction

Porous coordination polymers (PCPs) have recently attracted considerable attention because of their unique gas adsorption properties, controllable frameworks and pores, among other characteristics.[1-3] Because of the momentous effort that has been devoted to achieving large surface areas,[1] strong host-guest interactions[2] and high catalytic activities,[3] PCPs are now one of the most attractive materials for use as adsorbents and heterogeneous catalysts. One approach to creating new intelligent materials based on PCPs involves adding a guest sensing function by which the PCPs can indicate the kinds and/or amounts of adsorbed guest molecules by a *visual* response. Generally, the host-guest interactions in PCPs are not strong enough to affect the electronic transition in the host framework, which is usually observed in UV-Vis range. The utilization of chromophores and/or luminophores as bridging ligands is a promising method for realizing such intelligent absorbents. In fact, several groups have reported luminescent PCPs constructed from luminescent organic ligands; these PCPs show strongly guest-dependent emission properties that may be applicable to chemical sensors.[4-5]

Square-planar Pt(II)-diimine complexes are known to show interesting optical properties such as strong phosphorescence, colourful vapochromism etc.,[6-8] and accordingly, our recent efforts have focused on the development of multichromic PCPs constructed with Pt(II)-diimine-based metalloligands. The key factor determining the characteristic properties of these complexes is the metallophilic interaction between the $5dz^2$ orbitals of the Pt(II) ions which generates the emissive metal-metal-to-ligand charge transfer (MMLCT) state.[7] The energy level of the MMLCT state depends strongly on the distance between adjacent Pt(II) ions. By taking advantage of this feature, several groups have recently reported vapochromic Pt(II)-diimine complexes which can *visually* indicate the presence of chemical vapours.[8] This functionality is mainly based on the adsorption of vapour into the crystal lattice which induces changes in the metallophilic interaction. However, most vapochromic Pt(II)-diimine complexes are molecular solids assembled by relatively weak non-directional interactions such as van der Waals and Coulombic interactions, resulting in collapse of their vapour-accessible channels upon guest release. The design of guest

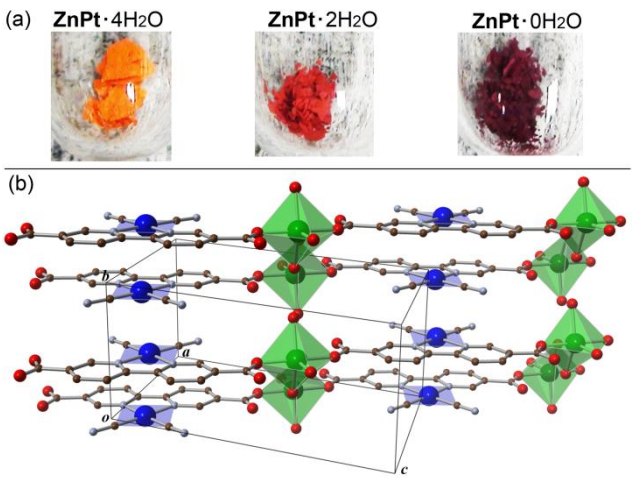

Fig. 1 (a) Bright field images from left of **ZnPt**·4H_2O, **ZnPt**·2H_2O and **ZnPt**·0H_2O. (b) Crystal structure of **ZnPt**·4H_2O. Coordination sphere of Pt(II) and Zn(II) ions are shown as blue planes and green polyhedra, respectively.[9, 13]

selectivity or recognition capabilities in such molecular systems, therefore, remains challenging.

To overcome these difficulties, we previously designed the bimetallic coordination polymer (CP), $\{[Zn(H_2O)_3][Pt(CN)_2(5,5'\text{-dcbpy})]\cdot H_2O\}_n$ (**ZnPt**·$4H_2O$; 5,5′-H_2dcbpy = 5,5′-dicarboxy-2,2′-bipyridine) and found that this CP can *visually* indicate the amount of adsorbed water molecules as shown in Figure 1.[9] However, **ZnPt** is capable of adsorbing only water vapour, possibly as a result of a lack of affinity between other vapour molecules and the Zn centre and/or coordinative saturation of the Zn ion. In this study, in order to enhance the host-guest interactions and to improve the vapour-adsorption properties of this class of CPs, we have synthesized the new bimetallic CPs, $\{M[Pt(CN)_2(5,5'\text{-dcbpy})]\}_n$ ($M = Mg^{2+}$, Ca^{2+}, Sr^{2+}, Ba^{2+}) by using alkaline-earth metal ions. The higher coordination numbers of alkaline-earth metal ions relative to that of the Zn^{2+} ion may enable us to design new intelligent adsorbents which *visually* indicate the type and amount of adsorbed guest molecules. We report herein the syntheses, chromic behaviours and adsorption properties of these bimetallic CPs and demonstrate that these CPs can adsorb not only water but also MeOH vapour accompanied by remarkable colour and luminescence changes.

Experimental

Syntheses

All starting materials, K_2PtCl_4 and 3-methylpyridine were used as received from commercial sources, and the solvents were used without purification. $Pt(CN)_2$,[10] 5,5′-H_2dcbpy,[11] and $K_2[Pt(CN)_2(5,5'\text{-dcbpy})]$[9] were prepared according to published methods. Elemental analysis was performed at the analysis centre in Hokkaido University.

$\{Mg[Pt(CN)_2(5,5'\text{-dcbpy})]\cdot 4H_2O\}_n$ (MgPt·$4H_2O$): $K_2[Pt(CN)_2(5,5'\text{-dcbpy})]$ (100 mg, 176 μmol) was dissolved in water (25 ml), and to this yellow solution, an aqueous solution (10 ml) of $Mg(NO_3)_2\cdot 6H_2O$ (46 mg, 179 μmol) was added. An orange precipitate formed immediately. After subsequent stirring for 1 h at room temperature, the solids were filtered off from the reaction mixture. The isolated precipitate was washed thoroughly with water and then dried in air for 1 day to afford the orange powder **MgPt**·$4H_2O$ (72 mg, 123 μmol) in 70 % yield. Elemental analysis calcd. for $C_{14}H_6N_4O_4PtMg\cdot 4H_2O$: C 28.71, H 2.41, N 9.42; found: C 28.51, H 2.53, N 9.57.

$\{Ca[Pt(CN)_2(5,5'\text{-dcbpy})]\cdot 4H_2O\}_n$ (CaPt·$4H_2O$): The **CaPt**·$4H_2O$ was synthesized by a similar procedure to **MgPt**·$4H_2O$, but using $CaCl_2$ instead of $Mg(NO_3)_2\cdot 6H_2O$. Yield: 78 mg, 74 % based on $K_2[Pt(CN)_2(5,5'\text{-dcbpy})]$. Elemental analysis calcd. for $C_{14}H_6N_4O_4PtCa\cdot 4H_2O$: C 27.96, H 2.35, N 9.32; found: C 28.28, H 2.32, N 9.00.

$\{Sr[Pt(CN)_2(5,5'\text{-dcbpy})]\cdot 4H_2O\}_n$ (SrPt·$4H_2O$): The **SrPt**·$4H_2O$ was synthesized by a similar procedure to **MgPt**·$4H_2O$, but using $SrCl_2\cdot 6H_2O$ instead of $Mg(NO_3)_2\cdot 6H_2O$. Yield: 102 mg, 89 % based on $K_2[Pt(CN)_2(5,5'\text{-dcbpy})]$. Elemental analysis calcd. for $C_{14}H_6N_4O_4PtSr\cdot 4H_2O$: C 25.91, H 2.17, N 8.63; found: C 25.47, H 2.23, N 8.54.

$\{Ba[Pt(CN)_2(5,5'\text{-dcbpy})]\cdot 4H_2O\}_n$ (BaPt·$4H_2O$): The **BaPt**·$4H_2O$ was synthesized by a similar procedure to **MgPt**·$4H_2O$, but using $Ba(NO_3)_2$ instead of $Mg(NO_3)_2\cdot 6H_2O$. Yield: 95 mg, 77 % based on $K_2[Pt(CN)_2(5,5'\text{-dcbpy})]$. Elemental analysis calcd. for $C_{14}H_6N_4O_4PtBa\cdot 4H_2O$: C 24.07, H 2.02, N 8.02; found: C 23.89, H 1.85, N 8.16.

Powder X-ray diffraction

Powder X-ray diffraction measurements were performed using a Rigaku SPD diffractometer at beamline BL-8B, Photon Factory, KEK, Japan. The wavelength of the synchrotron X-ray was 1.200(1) Å. The sample was placed in a glass capillary of 0.5 mmϕ diameter.

Photophysical measurements

Emission and excitation spectra were recorded under various conditions on a Jasco FP-6600 spectrofluorometer. The sample temperature was controlled by a JASCO ETC-273 Peltier-type temperature controller. About 1 mg of the sample was placed in a glass capillary with a diameter of 0.5 mmϕ. The slit widths of excitation and emission light were 5 and 6 nm, respectively. The luminescence quantum efficiency was recorded on a HAMAMATSU C9920-02 absolute photoluminescence quantum yield measurement system equipped with integrating sphere apparatus and 150 W CW Xenon light source. Emission lifetimes of all of the samples in the solid state were recorded using a HAMAMATSU C4780 Picosecond Fluorescence Lifetime Measurement System equipped with a nitrogen laser light source (λ = 337.1 nm).

Thermogravimetric analysis

Thermogravimetry and differential thermal analysis were performed using a Rigaku ThermoEvo TG8120 analyzer.

Adsorption Isotherms

The adsorption isotherms for water and MeOH vapours at 298 K were performed using an automatic volumetric adsorption apparatus (BELSORP-MAX and BELSORP-aqua; BEL Japan, Inc.)

Results and Discussion

Structures

The reactions between $K_2[Pt(CN)_2(5,5'\text{-dcbpy})]$ and alkaline-earth metal salts in aqueous solution led to immediate formation of the insoluble compounds, **MPt**·$4H_2O$. Because these very fast reactions made it difficult to synthesize single crystals suitable for single crystal X-ray structural determination, the insoluble compounds were characterized by powder X-ray diffraction (PXRD), IR spectroscopy and elemental analysis. Figure 2 shows the PXRD patterns of the four **MPt**·$4H_2O$ complexes at room temperature compared with that of **ZnPt**·$4H_2O$ for which single crystal XRD data had previously been obtained (Fig. 1). All of the observed PXRD patterns for **MPt**·$4H_2O$ are very similar to each other and seem to be identical with the pattern of **ZnPt**·$4H_2O$. Elemental analyses suggest that the hydration numbers of each of these CPs is four which is also the same as that of **ZnPt**·$4H_2O$. In addition, the IR spectra of **MPt**·$4H_2O$ are almost identical to the spectrum of **ZnPt**·$4H_2O$ (See Figure S1) including the splitting width of the ν(C≡N) bands, indicating that the cyano group does not coordinate to any of the metal ions.

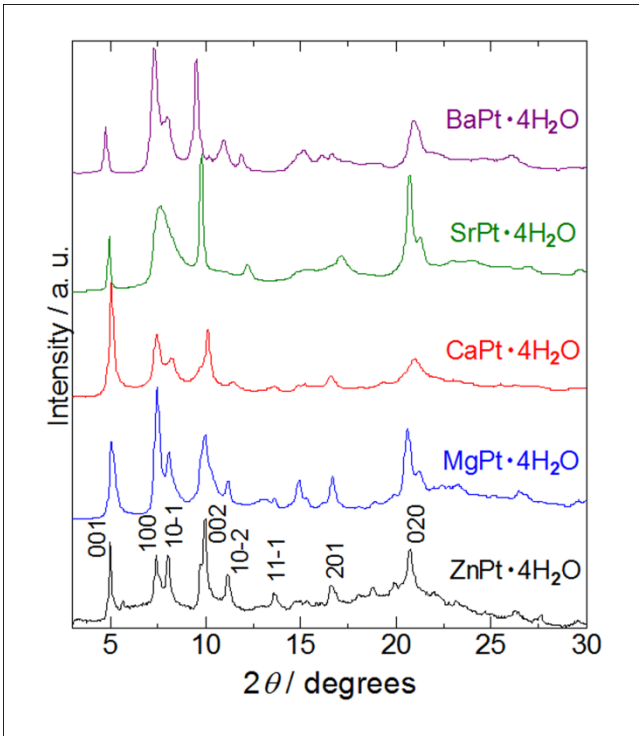

Fig. 2 PXRD patterns of **MPt**·4H_2O. (λ = 1.200(1) Å). Purple, green, red, blue, and black lines from the top show the pattern of, **BaPt**·4H_2O, **SrPt**·4H_2O, **CaPt**·4H_2O, **MgPt**·4H_2O, and **ZnPt**·4H_2O at 305 K, respectively. Indexes for main observed reflections of **ZnPt**·4H_2O are shown above the pattern.

Thus, it can be concluded that the structures of these CPs are isomorphous with **ZnPt**·4H_2O in terms of the one-dimensional infinite coordination chains formed by alternate arrangements of alkaline-earth metal ions M^{2+} and the Pt(II) metalloligands. Metallophilic interactions between adjacent Pt(II) ions are operative along the *b* axis, in the structure of **ZnPt**·4H_2O, with inter-nuclear distances of 3.309 Å, resulting in the orange colour of the solid. The almost isomorphic PXRD patterns of **MPt**·4H_2O may enable us to estimate the degree of metallophilic interaction between adjacent Pt ions in these CPs by comparing the locations of the (020) reflections. The (020) reflections were observed at 20.62°, 21.00°, 20.74°, and 20.94° for **MgPt**·4H_2O, **CaPt**·4H_2O, **SrPt**·4H_2O, and **BaPt**·4H_2O, respectively. The calculated Pt-Pt distances from the positions of the (020) reflections are as follows: **MgPt**·4H_2O: 3.40(3) Å, **CaPt**·4H_2O: 3.34(5) Å, **SrPt**·4H_2O: 3.39(3) Å, **BaPt**·4H_2O: 3.35(4) Å. These comparable distances are indicative of effective metallophilic interactions between Pt(II) ions in all of the CPs.

Thermochromic behaviour driven by water vapour adsorption/desorption

Because **ZnPt**·4H_2O exhibits thermochromic behaviour driven by the desorption/adsorption of water vapour,[9] the thermochromic behaviours of the **MPt**·4H_2O complexes were also examined and it was found that the variation of the M^{2+} ion in the series of **MPt**·4H_2O CPs affected their chromic behaviours considerably. Figure 3 shows the emission spectra of the **MPt**·4H_2O CPs at room temperature and at 373 K. The emission energies, lifetimes and quantum yields of **MPt**·4H_2O are summarized in Table 1. As expected from the Pt-Pt distances, observed emission energies of

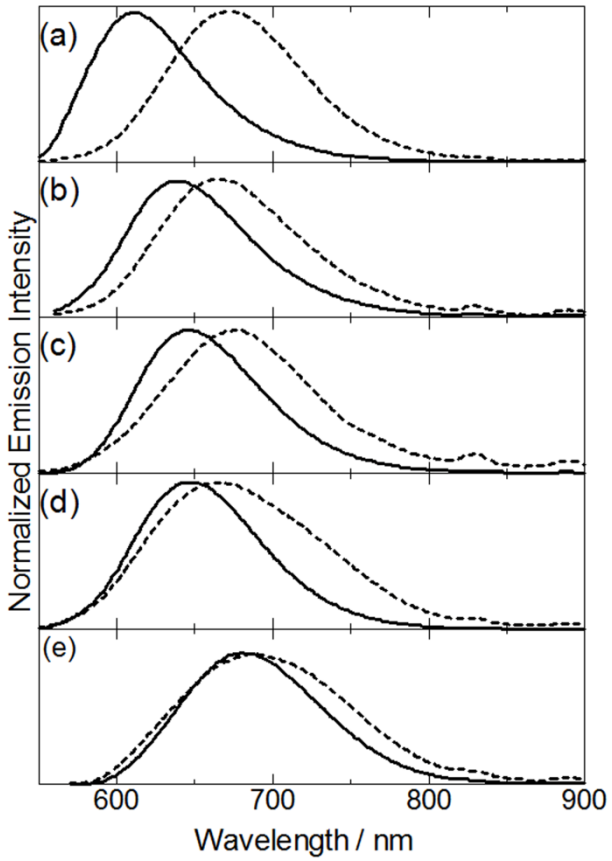

Fig. 3 Emission spectra of (a) **ZnPt**·4H_2O, (b) **MgPt**·4H_2O, (c) **CaPt**·4H_2O, (d) **SrPt**·4H_2O, and (e) **BaPt**·4H_2O at room temperature (solid lines) and 373 K (broken lines).

Table 1 Photophysical data of **MPt**·4H_2O

Complex	$\lambda_{em.}$ (RT) / nm	$\lambda_{em.}$(373 K) / nm	Φ [a]	τ_{em} / ns [a]	Ionic radius of M^{2+} ion / Å [b]
ZnPt	611	674	0.06	25	0.88
MgPt	639	664	0.05	31	0.86
CaPt	646	675	0.05	46	1.14
SrPt	646	666	0.12	69	1.32
BaPt	680	687	0.07	52	1.49

[a] At room temperature. [b] In 6-coordinated structure. see ref. No.14.

these **MPt**·4H_2O CPs are in the energy range of emission from a ^{3}MMLCT (triplet metal-metal-to-ligand charge transfer) state which is commonly observed for Pt(II)-diimine complexes with effective Pt-Pt interaction, for example the ^{3}MMLCT emission of [Pt(CN)$_2$(4,4'-H_2dcbpy)] at 614 nm.[12] The emission bands of all of the CPs shifted to longer wavelengths when the temperature was increased to 373 K. The original emission spectra at room temperature were regained after exposure of the complexes to water vapour at room temperature. Interestingly, the extent of the red shifts induced by increasing the temperature followed the order: **ZnPt**·4H_2O (1430 cm^{-1}) > **CaPt**·4H_2O (641 cm^{-1}) > **MgPt**·4H_2O (589 cm^{-1}) > **SrPt**·4H_2O (372 cm^{-1}) > **BaPt**·4H_2O (85 cm^{-1}) and the maximum emission wavelength for all of the complexes after heating were comparable with each other in the region of 670 nm. It had been previously determined that the red shift observed in **ZnPt**·4H_2O was due to the release of water molecules from the compound.[9] Thermogravimetric analyses

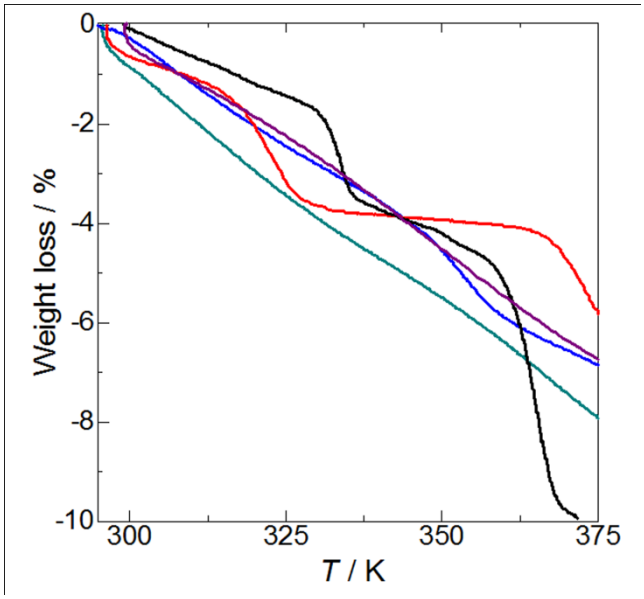

Fig. 4 Thermogravimetric curves of **MPt**·4H_2O. Black, blue, red, green, purple lines show the TG curves of **ZnPt**·4H_2O, **MgPt**·4H_2O, **CaPt**·4H_2O, **SrPt**·4H_2O, and **BaPt**·4H_2O respectively. (1 K min^{-1} heating, Ar flow rate: 300 ml min^{-1})

were performed in order to clarify the relationship between the red shift in the luminescence spectrum and the amount of water desorbed. As shown in Figure 4, the alkaline-earth metal CPs also released water molecules upon increasing the temperature. The observed weight loss for each **MPt**·4H_2O (6.86% for **MgPt**·4H_2O, 5.79% for **CaPt**·4H_2O, 7.92% for **SrPt**·4H_2O, 6.72% for **BaPt**·4H_2O) was smaller than that of **ZnPt**·4H_2O (9.95 %), which implies that some of the water molecules remained in the structures even at 375 K. The hydration numbers at 375 K of these CPs were estimated from the weight losses to be about 2.0 for **MgPt** and **CaPt**, 1.5 for **SrPt** and **BaPt**, and 0.5 for **ZnPt**. This result suggests two facts as follows: firstly, the four CPs with alkaline-earth metal ions bind water molecules more strongly than in **ZnPt**·4H_2O, which is substantiated by the water-vapour adsorption isotherms (discussed below). Secondly, **MgPt**·4H_2O and **CaPt**·4H_2O showed a larger red shift than that observed for **SrPt**·4H_2O or **BaPt**·4H_2O in spite of the smaller amount of water desorption. These differences suggest that the intermolecular Pt-Pt distance can be modified by water desorption more effectively in **MgPt**·4H_2O and **CaPt**·4H_2O than in **SrPt**·4H_2O and **BaPt**·4H_2O.

Solid-state (suspension) solvatochromic behaviours

Because **ZnPt**·4H_2O showed solid state (*insoluble*) solvatochromic behaviour driven by the release of water molecules in highly-polar liquids,[9] the solvent responsive behaviour of **MPt**·4H_2O was also examined. Note that the solubilities of these CPs in common solvents used herein are negligibly small. Figure 5 shows the solid state emission spectral changes of **MPt**·4H_2O when immersed in various solvents. The observed emission maxima of **MPt**·4H_2O in the suspended states and the dielectric constants of the solvents are summarized in Table 2. As shown in the mainframe and inset pictures of Figure 5, **MgPt**·4H_2O and **CaPt**·4H_2O exhibited drastic colour and luminescence changes in highly-polar liquids such as MeOH and

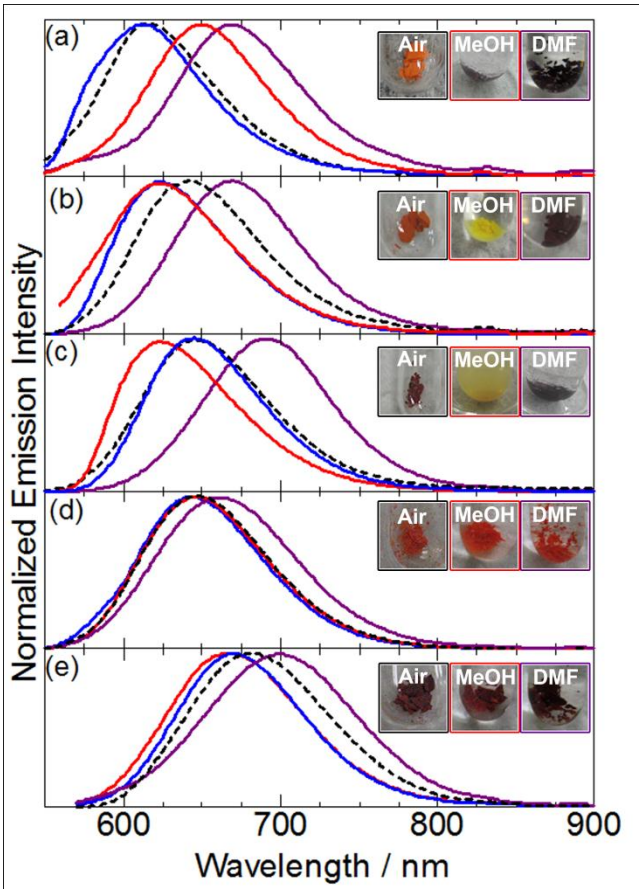

Fig. 5 Emission spectra of (a) **ZnPt**·4H_2O, (b) **MgPt**·4H_2O, (c) **CaPt**·4H_2O, (d) **SrPt**·4H_2O, and (e) **BaPt**·4H_2O. Black-broken, blue-, red-, and purple-solid lines show the spectrum of **MPt**·4H_2O in air, immersed in water, MeOH, and DMF, respectively. Inset pictures from left show the bright field images of **MPt**4H_2O in air, immersed in MeOH and DMF.

dimethylformamide (DMF). Similar red shift was observed in the UV-Vis diffuse reflectance spectrum of the **MgPt**·4H_2O suspended in DMF (see Figure S4). In contrast, the colour changes observed for **SrPt**·4H_2O and **BaPt**·4H_2O were less distinctive than in the other two complexes. The emission maxima of the **MPt**·4H_2O CPs changed only marginally upon immersion in non-polar solvents such as hexane and toluene. Basically, the emission bands of the **MPt**·4H_2O CPs shifted to longer wavelengths upon immersion in highly-polar liquids, except for water and MeOH, and the observed red-shifts seem to be proportional to the dielectric constants of the liquids (see Figure S2). In addition, these emission shifts were negligible in the solvents that contained 10% or more water (see Figure S3) and none of the **MPt**·4H_2O CPs are able to adsorb the vapours of any of these liquids except for water and MeOH (discussed below). Thus, these solid state solvatochromic behaviours are thought to originate from the extraction of water molecules bound in the crystal lattice into highly-polar solvents as shown in Schemes 1(a) and (b), leading to the red shift of the ^{3}MMLCT emission generated by enhancing the Pt-Pt interaction. The relatively large red-shifts observed for every **MPt** in low-polar THF suspension are probably due to the high affinity of THF to water (e.g. the very large solubility of THF to water). The thermochromic behaviours as well as the observed red shifts of

Table 2 Observed emission maxima ($\lambda_{max.}$) of complexes **MPt**·$4H_2O$ immersed in various liquids.

liquid	dielectric constant [a]	$\lambda_{max.}$ / nm				
		ZnPt	**MgPt**	**CaPt**	**SrPt**	**BaPt**
In air (303 K)	1.0	614	639	647	648	683
H_2O	78.3	612	625	645	643	671
n-Hexane	2.0	613	637	651	648	683
Heptane	1.924	623	637	657	-	-
Toluene	2.379	625	641	659	650	682
Cyclohexane	2.015	626	638	658	-	-
Ethylacetate	6.0	626	649	655	-	-
Benzene	2.274	627	638	655	-	-
$CHCl_3$	4.806	628	638	662	649	-
Et_2O	4.335	630	649	650	-	-
1,4-Dioxane	2.102	640	656	671	-	-
1-Butanol	17.51	641	649	672	-	-
EtOH	24.55	646	646	669	653	694
CH_2Cl_2	7.77	649	638	647	-	-
MeOH	32.6	650	623	623	648	667
2-PrOH	19.92	652	644	664	-	-
Acetone	20.7	652	645	661	653	689
1-Pentanol	13.9	656	650	673	-	-
THF	7.5	665	658	677	659	696
MeCN	37.5	667	669	678	657	696
DMF	38	669	669	690	663	698
In air (373 K)	1.0	673	664	675	664	687

[a] See ref. No15.

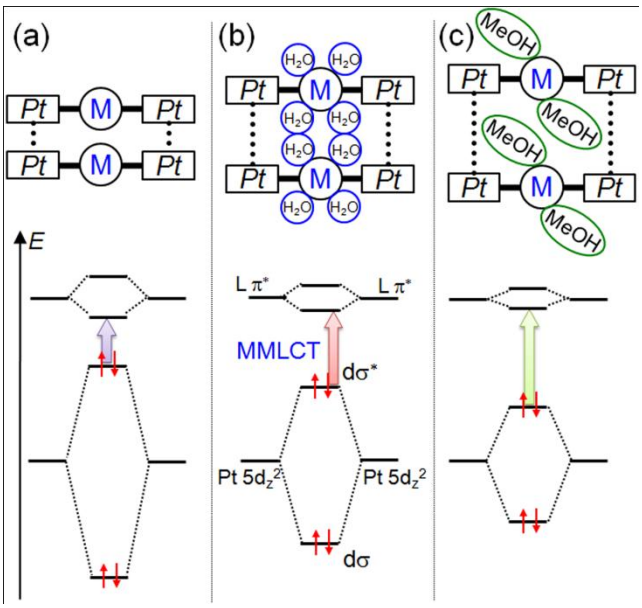

Scheme 1 Possible mechanism of chromic behaviours of **MPt** CPs. Upper and lower sections show schematic structural representations and energy diagrams of (a) anhydrous **MPt**, (b) tetrahydrated **MPt**·$4H_2O$ and (c) MeOH adsorbed state.

the alkaline-earth **MPt**·$4H_2O$ CPs were smaller than those of **ZnPt**·$4H_2O$. This difference may be due to the strong binding of water molecules at the bridging M^{2+} ions. An interesting difference between **ZnPt**·$4H_2O$ and alkaline-earth metal CPs was also observed in the water and MeOH suspended states. The emission bands of **MgPt**·$4H_2O$ and **BaPt**·$4H_2O$ shifted by 14 and 12 nm (351 and 262 cm^{-1}), respectively, to lower wavelength (higher energy) upon immersion in water, whereas the emission bands of the Zn, Ca, and Sr complexes did not change

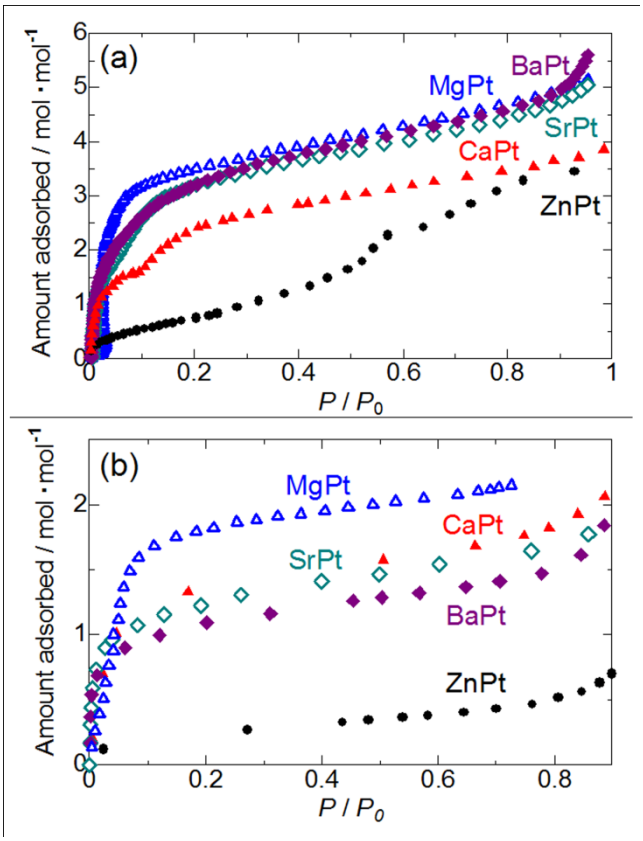

Fig. 6 (a) Water and (b) MeOH vapour-adsorption isotherms of **MPt** at 298 K.

significantly. In addition, the emission bands of **MgPt**·$4H_2O$, **CaPt**·$4H_2O$ and **BaPt**·$4H_2O$ shifted by 16, 24 and 16 nm (402, 596 and 351 cm^{-1}), respectively, to lower wavelength (higher energy) upon immersion in MeOH. Similar blue shift was observed in the UV-Vis diffuse reflectance spectrum of the **MgPt**·$4H_2O$ suspended in MeOH (see Figure S4). Taking into account the fact that the ^{3}MMLCT emission band of **ZnPt**·$4H_2O$ showed only red shifts, the observed blue shifts for **MgPt**·$4H_2O$, **CaPt**·$4H_2O$ and **BaPt**·$4H_2O$ reflect the substitution effect of the bridging M^{2+} ions. Judging from the vapour-adsorption isotherms, these CPs can adsorb about 2 mol·mol^{-1} of MeOH vapour (see below). Thus, this adsorption of additional water or MeOH would elongate the Pt-Pt distances, resulting in the blue shift of the ^{3}MMLCT emission(Scheme 1(c)).

Vapour-adsorption properties

As mentioned in the Introduction, **ZnPt** can adsorb only water vapour.[9] The vapour adsorption isotherms of **MPt** were measured in order to evaluate the substitution effect of the bridging metal ions on the vapour-adsorption properties. Prior to these measurements, the samples were dried at 373 K under vacuum. The observed weight losses in this drying process (13%, 13%, 11% and 10% for **MgPt**·$4H_2O$, **CaPt**·$4H_2O$, **SrPt**·$4H_2O$, and **BaPt**·$4H_2O$, respectively) suggest that each **MPt**·$4H_2O$ CP released all of its water molecules to form anhydrous **MPt**. Figure 6(a) shows the water-vapour-adsorption isotherms of **MPt** at 298 K. All of the CPs can adsorb water vapour from 4 to 5 mol·mol^{-1} at the saturated water vapour pressure. It should be emphasized that all of the **MPt** CPs except for **ZnPt** adsorbed

water vapour in the very low pressure region below 0.1 P/P_0, suggesting that the host-guest interaction between the **MPt** framework and water molecules is stronger than in **ZnPt**, consistent with the TG results. In addition, the saturated adsorption amounts are also different: 4 mol·mol^{-1} for **CaPt** and 5 mol·mol^{-1} for **MgPt**, **SrPt**, and **BaPt**. In other words, **MgPt**·4H_2O, **SrPt**·4H_2O, and **BaPt**·4H_2O are able to adsorb an additional 1 mol·mol^{-1} of water vapour to form the pentahydrate, **MPt**·5H_2O. The formation of these pentahydrates may account for the origin of the slight blue shifts in the luminescence spectra of **MgPt**·4H_2O and **BaPt**·4H_2O immersed in water. In other words, the Pt-Pt distances of these CPs elongated upon adsorption of additional water, in the water suspension, resulting in the blue shift of the ^{3}MMLCT emission. Figure 6(b) shows the MeOH-vapour-adsorption isotherms of **MPt** at 298 K. In contrast to the fact that **ZnPt** cannot adsorb MeOH vapour at all, **MgPt**, **CaPt**, **SrPt**, and **BaPt** can adsorb MeOH vapour at low pressure. The saturated adsorption amounts are about 2 mol·mol^{-1} for each CP. The emission spectrum of anhydrous **CaPt** upon exposure to MeOH vapour was almost identical to the spectrum obtained from the **CaPt**·4H_2O in MeOH suspension (see Figure S3). Thus, we believe that the blue-shifts observed in the MeOH suspensions of **MgPt**·4H_2O and **CaPt**·4H_2O originate from the guest exchange reaction of water with MeOH as shown in Scheme 1(c). Although we also measured the EtOH vapour adsorption isotherms for these CPs, the adsorbed amounts were negligibly small for all of the CPs (see Figure S5).

Substitution effect of the bridging metal ions

As discussed above, the chromic behaviours and vapour-adsorption properties of **MPt**·4H_2O depend strongly on the bridging metal ions in spite of their isomorphous structures. In this section, we discuss the substitution effect of the bridging metal ions. In the case of **ZnPt**·4H_2O, the Zn^{2+} ion in the structure acted as the water adsorption site and the coordination geometry of Zn^{2+} ion changed by desorption of the all water molecules from 5-coordinated trigonal-bipyramid to 4-coordinated tetrahedron accompanied by the change of coordination mode of the carboxyl group from the monodentate to bidentate fashion.[9] Because the four **MPt**·4H_2O CPs are thought to be isomorphous with **ZnPt**·4H_2O, the bridging alkaline-earth metal ions should also act as the vapour-adsorption sites. All anhydrous **MPt** CPs can adsorb MeOH vapour in contrast to the lack of adsorption ability of **ZnPt** to MeOH vapour. This adsorption capability for MeOH vapour may originate from the strong coordination abilities of the coordinatively-unsaturated M^{2+} ions. Although alkaline-earth metal ions rarely adopt the four-coordinate structure, the Zn^{2+} ion is well known to be able to adopt the four-coordinate tetrahedral structure. Consequently, the bridging M^{2+} ion in the anhydrous **MPt** would have strong adsorption ability on the basis of the coordinatively-unsaturated structure. In fact, the adsorption amounts of water and MeOH vapours for all of the **MPt** CPs increased sharply in the very low vapour pressure region, suggesting chemical adsorption.

Remarkable differences in the thermochromic and suspended-state solvatochromic shifts were also observed for the four CPs with alkaline-earth metal ions, demonstrating the dependence on the M^{2+} ion. Although **MgPt**·4H_2O and **CaPt**·4H_2O showed relatively large chromic shifts, **SrPt**·4H_2O and **BaPt**·4H_2O exhibited minimal chromic shifts. This tendency is probably owing to the relatively larger volume occupied by water molecules in the unit cells of **MgPt**·4H_2O and **CaPt**·4H_2O than those of **SrPt**·4H_2O and **BaPt**·4H_2O. The larger **M** ions make the volume occupied by water molecules relatively smaller, resulting in smaller modifications in the Pt-Pt distances induced by water desorption. These relatively rigid structures of **SrPt**·4H_2O and **BaPt**·4H_2O may contribute to their higher luminescence quantum yields and longer lifetimes than those of the other **MPt**. The lower quantum yield of **BaPt**·4H_2O than that of **SrPt**·4H_2O would be due to the lower emission energy than that of **SrPt**·4H_2O. In addition, the observed water-vapour adsorption amounts (*ca.* 5 mol·mol^{-1}) of **MgPt**, **SrPt** and **BaPt** are larger than **CaPt** (*ca.* 4 mol·mol^{-1})**.** The larger water-vapour-adsorption capacity of **MgPt** (*ca.* 5 mol·mol^{-1}) is probably due to the large hydration enthalpy of the Mg^{2+} ion, whereas the increased adsorption capacity of **SrPt** and **BaPt** may originate from the higher coordination numbers of these heavier alkaline-earth metal ions.

The selective vapour adsorption capacity of the CPs (lack of vapour-adsorption ability for vapours other than water and MeOH) may be attributed to instability of vapour-adsorbed structure in these CPs. The lack of adsorption capability of every **MPt** with alkaline-earth metal ion for EtOH vapour suggests that the larger coordinating vapour molecules than MeOH would not be able to enter the vapour accessible channels around the M^{2+} ions, resulting in the negligible small vapour uptake. Thus, the adsorption properties of **MPt** depend strongly on the kinds of bridging metal ions which produces remarkable effects on the chromic behaviours of the complexes.

Conclusions

Four new coordination polymers, {M[Pt(CN)$_2$(5,5′-dcbpy)]·4H_2O}$_n$ (M = Mg^{2+}, Ca^{2+}, Sr^{2+}, Ba^{2+}; 5,5′-H_2dcbpy = 5,5′-dicarboxy-2,2′-bipyridine) were successfully synthesized using alkaline-metal ions and the luminophoric Pt(II)-diimine metalloligand, [Pt(CN)$_2$(5,5′-dcbpy)]$^{2-}$. The structures of all of the CPs are essentially isomorphous with {Zn[Pt(CN)$_2$(5,5′-dcbpy)]·4H_2O}$_n$, which consists of one-dimensional polymeric chains formed by an alternating arrangement of M^{2+} ions and the [Pt(CN)$_2$(5,5′-dcbpy)]$^{2-}$ metalloligand, with effective metallophilic interaction between Pt(II) ions. The vapour-adsorption capability of this system was remarkably altered by replacement of Zn^{2+} ion with alkaline-earth metal ions, resulting in selective adsorption for water and MeOH vapours. These CPs exhibit interesting thermochromic and solid-state (suspension) solvatochromic behaviours driven by water or MeOH adsorption/desorption. Variation of the bridging metal ions produced significant effects on the chromic behaviours in spite of the isomorphous nature of the structures, i.e., the chromic shift observed for CPs with larger alkaline-earth metal ions are remarkably smaller than those for CPs with smaller ions. Further studies on the synthesis of novel CPs composed of other Pt(II)-diimine-based metalloligands to achieve both gas sensing and adsorption functions are now in progress.

Acknowledgements

This work is supported by a Grant-in-Aid for Scientific Research, Photochromism (No.471), Coordination Programming (No. 2107), Young Scientists (B) (19750050) and the Global COE Program (Project No. B01: Catalysis as the Basis for Innovation in Materials Science) from MEXT, Japan.

Notes and references

[a] *Division of Chemistry, Faculty of Science, Hokkaido University, North-10 West-8, Kita-ku, Sapporo 060-0810, Japan. Fax: 81-11-706-3447; Tel:81-11-706-3817; E-mail: akoba@sci.hokudai.ac.jp (A.K.), mkato@sci.hokudai.ac.jp (M. K.)*

[b] *Research Institute for Electronic Science, Hokkaido University, North-20, West-10, Kita-ku, Sapporo 001-0020, Japan*

† Electronic Supplementary Information (ESI) available: IR spectra of **MPt**·$4H_2O$, plots of the emission energies of **MPt**·$4H_2O$ against dielectic constants of the soaking liquids, emission spectral changes of **CaPt**·$4H_2O$ soaked in water-containing solvents and under exposure to MeOH vapor, UV-Vis diffuse reflectrance spectra of **MgPt**·$4H_2O$ in air, suspended in DMF and MeOH, and EtOH vapour-adsorption isotherms of **MPt** at 298 K. See DOI: 10.1039/b000000x/

1 G. J. Halder, C. J. Kepert, B. Moubaraki, K.S. Murray, J. D. Cashion, *Science* 2002, **298**, 1762.; S. Kitagawa, R. Kitaura, S. Noro, *Angew. Chem. Int. Ed.* 2004, **43**, 2334.; R. Matsuda, R. Kitaura, S. Kitagawa, Y. Kubota, R. V. Belosludov, T. C. Kobayashi, H. Sakamoto, T. Chiba, M. Takata, Y. Kawazoe, Y. Mita, *Nature* 2005, **436**, 238.; O. M. Yaghi, *Nat. Mater.* 2007, **6**, 92.; B. D. Chandler, G. D. Enright, K. A. Udachin, S. Pawsey, J. A. Ripmeester, D. T. Cramb, G. K. H. Shimizu, *Nat. Mater.* 2008, **7**, 229.; D. Tanaka, K. Nakagawa, M. Higuchi, S. Horike, Y. Kubota, T. C. Kobayashi, M. Takata, S. Kitagawa, *Angew. Chem. Int. Ed.* 2008, **47**, 3914.; J.-R. Li, R. J. Kuppler, H.-C. Zhou, *Chem. Soc. Rev.* 2009, **38**, 1477.; S. Horike, S. Shimomura, S. Kitagawa, *Nat. Chem.* 2009, **1**, 695.; M. Higuchi, D. Tanaka, S. Horike, H. Sakamoto, K. Nakamura, Y. Takashima, Y. Hijikata, N. Yanai, J. Kim, K. Kato, Y. Kubota, M. Takata, S. Kitagawa, *J. Am. Chem. Soc.* 2009, **131**, 10336.; T. Fukushima, S. Horike, Y. Inabushi, K. Nakagawa, Y. Kubota, M. Takata, S. Kitagawa, *Angew. Chem. Int. Ed.* 2010, **49**, 4820.

2 H. Li, M. Eddaoudi, M. O'Keeffe, O. M. Yaghi, *Nature* 1999, **402**, 276.; M. Eddaoudi, D. B. Moler, H. Li, B. Chen, T. M. Reineke, M. O'Keeffe, O. M. Yaghi, *Acc. Chem. Res.* 2001, **34**, 319.; N. L. Rosi, J. Kim. M. Eddaoudi, B. Chen, M. O'Keeffe, O. M. Yaghi, *J. Am. Chem. Soc.* 2005, **127**, 1504.; T. Louseau, G. Férey, *Fluor. Chem.* 2007, **128**, 413.; R. Banerjee, A. Phan. B. Wang, C. Knobler, H. Furukawa, M. O'Keeffe, O. M. Yaghi, *Science* 2008, **319**, 939.; G. Férey, C. Serre, *Chem. Soc. Rev.* **2009**, *38*, 1380.; D. J. Tranchemontagne, J. L. Mendoza-Cortes, M. O'Keeffe, O. M. Yaghi, *Chem. Soc. Rev.* 2009, **38**, 1257.

3 D.-Y. Hong, Y. K. Hwang, C. Serre, G. Férey, J.-S. Chang, *Adv. Funct. Mater.* 2009, **19**, 1537.; A. M. Shultz, O. K. Farha,J. T. Hupp, S. T. Nguyen, *J. Am. Chem. Soc.* 2009, **131**, 4204.; L. Yang, S. Kinoshita, T. Yamada, S. Kanda, H. Kitagawa, M. Tokunaga, T. Ishimoto, T. Ogura, R. Nagumo, A. Miyamoto, M. Koyama, *Angew. Chem. Int. Ed.* 2010, **49**, 5348.; A. Dhakshinamoorthy, M. Alvaro, H. Garcia, *Chem. Commun.* 2010, **46**, 6476.

4 B. Chen, L. Wang, F. Zapata, G. Qian, E. B. Lobkovsky, *J. Am. Chem. Soc.* 2008, **130**, 6718.; M. D. Allendorf, C. A. Bauer, R. K. Bhakta, R. J. T. Houk, *Chem. Soc. Rev.* 2009, **38**, 1330.; K. C. Stylianou, R. Heck, S. Y. Chong, J. Bacsa, J. T. A. Jones, Y. Z. Khimyak, D. Bradshaw, M. J. Rosseinsky, *J. Am. Chem. Soc.* 2010, **132**, 4119.

5 Reineke, T. M.; Eddaoudi, M.; Fehr, M.; Kelley, D.; Yaghi, O. M. *J. Am. Chem. Soc.* 1999, **121**, 1651.; B. D. Chandler, D. T. Cramb,G. K. H. Shimizu, G. K. H. *J. Am. Chem. Soc.* 2006, **128**, 10403.; White, K. A.; Chengelis, D. A.; Gogick, K. A.; Stehman, J.; Rosi, N. L.; Petoud, S. *J. Am. Chem. Soc.* 2009, **131**, 18069.; Lin, Z.-J.; Xu, B.; Liu, T.-F.; Cao, M.-N.; Lu, J.; Cao, R. *Eur. J. Inorg. Chem.* 2010, 3842.

6 T. W. Thomas and A. E. Underhill, *Chem. Soc. Rev.*, 1972, **1**, 99; L. Chassot, E. Muller, A. V. Zelewsky, *Inorg. Chem.*, 1984, **23**, 4249-4253. ; R. Ballardini, G. Varani, M. T. Indelli and F. Scandola, *Inorg. Chem.*, 1986, **25**, 3858.; C.-M. Che, L.-Y. He, C.-K. Poon and T. C. W. Mak, *Inorg. Chem.*, 1989, **28**, 3081.; V. M. Miskowski and V. H. Houlding, *Inorg. Chem.*, 1989, **28**, 1529.; J. A. Zuleta, M. S. Burberry and R. Eisenberg, *Coord. Chem. Rev.*, 1990, **97**, 47.; V. H. Houlding and V. M. Miskowski, *Coord. Chem. Rev.*, 1991, **111**, 145.; S. D. Cummings and R. Eisenberg, *J. Am. Chem. Soc.*, 1996, **116**, 1949.; S. Huertas, M. Hissler, J. E. McGarrah, R. J. Lachicotte and R. Eisenberg, *Inorg. Chem.*, 2001, **40**, 1183.; A. Islam, H. Sugihara, K. Hara, L. P. Singh, R. Katoh, M. Yanagida, Y. Takahashi, S. Murata, H. Arakawa, G. Fujihashi, *Inorg. Chem.*, 2001, **40**, 5371.; J. Zhang, P. Du, J. Schneider, P. Jarosz, R. Eisenberg, *J. Am. Chem. Soc.*, 2007, **129**, 7726.; M. Kato, Y. Shishido, Y. Ishida and S. Kishi, *Chem. Lett.*, 2008, **37**, 16.

7 J. A. Bailey, M. G. Hill, R. E. Marsh, V. M. Miskowski, W. P. Schaefer and H. B. Gray, *Inorg. Chem.*, 1995, **34**, 4591. ; V. W.-W. Yam, K. M.-C. Wong and N. Zhu, *J. Am. Chem. Soc.*, 2002, **124**, 6506.; S.-Y. Lai, H.-W. Lam, W. Lu, K.-K. Cheung and C.-M. Che, *Organometallics*, 2002, **21**, 226.; V. W.-W. Yam, K. H.-Y. Chan, K. M.-C. Wong and N. Zhu, *Chem. Eur. J.*, 2005, **11**, 4535-4543.; A. Y.-Y. Tam, K. M.-C. Wong, G. Wang and V. W.-W. Yam, *Chem. Commun.*, 2007, 2028.

8 C. L. Exstrom, J. R. Sowa, C. A. Daws, D. Janzen, K. R. Mann, *Chem. Mater.* 1995, **7**, 15; M. Albrecht, M. Lutz, A. L. Spek, G. Koten, *Nature*, 2000, **406**, 970; M. H. Keefe, K. D. Benkstein, J. T. Hupp, *Coord. Chem. Rev.*, 2000, **205**, 201; S. M. Drew, D. E. Janzen, C. E. Buss, D. I. MacEwan, K. M. Dublin, K. R. Mann, *J. Am. Chem. Soc.* 2001, **123**, 8414; S. Kishi and M. Kato, *Mol. Cryst. Liq. Cryst.*, 2002, **379**, 303.; M. Kato, A. Omura, A. Toshikawa, S. Kishi and Y. Sugimoto, *Angew, Chem. Int. Ed.*, 2002, **41**, 3183.; T. J. Wadas, Q.-M Wang, Y.-J. Kim, C. Flaschenreim, T. N. Blanton, R. Eisenberg, *J. Am. Chem. Soc.* 2004, **126**, 16841; L. J. Grove, J. M. Rennekamp, H. Jude, W. B. Connick, *J. Am. Chem. Soc.* 2004, **126**, 1594. ; S. C. F. Kui, S. S.-Y. Chui, C.–M. Che, N. Zhu, *J. Am. Chem. Soc.* 2006, **128**, 8297.; M. Kato, *Bull. Chem. Soc. Jpn.* 2007, **80**, 287.; J. Fornies, S. Fuertes, J. A. Lopez, A. Martin, V. Sicilia, *Inorg. Chem.*, 2008, **47**, 7188; M. L. Muro, C. A. Daws, F. N. Castellano, *Chem. Commun.*, 2008, 6134.; J. Fornies, S. Fuertes, J. A. Lopez, A. Martin and V. Sicilia, *Inorg. Chem.*, 2008, **47**, 7166.; A. Kobayashi, Y. Fukuzawa, S. Noro, T. Nakamura and M. Kato, *Chem. Lett.* 2009, **38**, 998.; A. Kobayashi, T. Yonemura and M. Kato, *Eur. J. Inorg. Chem.*, 2010, 2465.; A. Kobayashi, M. Dosen, M. Chang, K. Nakajima, S. Noro and M. Kato, *J. Am. Chem. Soc.* 2010, **132**, 15286.

9 A. Kobayashi, H. Hara, S. Noro and M. Kato, *Dalton Trans.* 2010, **39**, 3400.

10 A. Avshu and A. M. Parkins, *J. Chem. Research*, 1984, 2201.

11 K. C. Szeto, K. O. Kongshaug, S. Jakobsen, M. Tilset, K. O. Lillerud, *Dalton Trans.*, 2008, 2054-2060; H. F.M. Nelissen, M. C. Feiters, R. J. M. Nolte, *J. Org. Chem.*, 2002, **67**, 5901.

12 M. Kato, S. Kishi, Y. Wakamatsu, Y. Sugi, Y. Osamura, T. Koshiyama, M. Hasegawa, *Chem. Lett.*, 2005, **34**, 1368-1369.

13 The structure was drawn by VESTA computer program. K. Momma and F. Izumi, "VESTA: a three-dimensional visualization system for electronic and structural analysis," *J. Appl. Crystallogr.*, 2008, **41**, 653.

14 N. Hirota, in *Handbook of Chemistry*, ed. K. Hatake, Maruzen, Tokyo, Basic 4th Ed. 1984, Vol. 2, ch. 15, pp. 717-718.

15 N. Hirota, in *Handbook of Chemistry*, ed. K. Hatake, Maruzen, Tokyo, Basic 4th Ed. 1984, Vol. 2, ch. 13, pp. 501-506,.